Pergamon

Geochimica et Cosmochimica Acta, Vol. 58, No. 22, pp. 4831–4839, 1994

0016-7037/94 $6.00 + .00

0016-7037(94)00257-6

The solubility of quartz in H_2O in the lower crust and upper mantle

CRAIG E. MANNING

Department of Earth and Space Sciences, University of California, Los Angeles, Los Angeles, CA 90024-1567, USA

(*Received February* 16, 1994; *accepted in revised form July* 8, 1994)

Abstract—The solubility of quartz in H_2O has been determined experimentally from 5 to 20 kb and 500 to 900°C. The results double the pressure range over which the molality of aqueous silica ($m_{SiO_{2(aq)}}$) has been determined and lead to more accurate estimates of quartz solubility in H_2O below 5 kb because of the rapid-quench methods employed. At constant temperature, log $m_{SiO_{2(aq)}}$ increases with increasing pressure and $(\partial \log m_{SiO_{2(aq)}}/\partial P)_T$ decreases with increasing pressure. Comparison of the new data with previous low-pressure experiments demonstrates that isothermal values of log $m_{SiO_{2(aq)}}$ increase linearly with increasing log ρ_{H_2O} between 200 and 900°C. This observation was used to derive the following expression for the equilibrium constant (K) of the reaction quartz = $SiO_{2(aq)}$:

$$\log K = 4.2620 - \frac{5764.2}{T} + \frac{1.7513 \times 10^6}{T^2} - \frac{2.2869 \times 10^8}{T^3} + \left[2.8454 - \frac{1006.9}{T} + \frac{3.5689 \times 10^5}{T^2}\right] \log \rho_{H_2O},$$

where log K = log $m_{SiO_{2(aq)}}$. The equation agrees well with previous results, while accurately reproducing measured quartz solubilities over a much wider range in pressure and temperature, from 25°C and 1 bar to the conditions of this study. If the isothermal variation of log $m_{SiO_{2(aq)}}$ with log ρ_{H_2O} is assumed to be linear, the results can be extrapolated to >20 kb. The equation allows evaluation of aqueous silica transport in Barrovian metamorphic belts, subduction zones, and metasomatized magma source-regions in the mantle.

INTRODUCTION

THE SOLUBILITY OF QUARTZ in aqueous solutions is of fundamental importance to geochemistry and petrology. Concentrations of aqueous Si in equilibrium with quartz increase with pressure and temperature from ~0.1 wt% in pure H_2O at conditions of low-grade metamorphism and geothermal systems to >5 wt% at conditions of high-grade metamorphism in the middle crust (KENNEDY, 1950; MOREY and HESSELGESSER, 1951; WYART and SABATIER, 1955; KHITAROV, 1956; KITAHARA, 1960; VAN LIER et al., 1960; MOREY et al., 1962; SIEVER, 1962; WEILL and FYFE, 1964; ANDERSON and BURNHAM, 1965, 1967; HEITMANN, 1965; CRERAR and ANDERSON, 1971; HEMLEY et al., 1980; WALTHER and ORVILLE, 1983; RIMSTIDT, 1984). The magnitude and variation of quartz solubility in H_2O results in a strong potential for local to large-scale redistribution of Si during fluid-rock interaction in diverse geologic environments (e.g., WOOD and WALTHER, 1986).

Because quartz solubility increases with pressure at a given temperature, Si metasomatism is particularly important in metamorphic and igneous processes at high pressures. However, virtually all experimental studies of quartz solubility have been carried out below ~4 kb. The seminal study of ANDERSON and BURNHAM (1965) has provided the only data with which to evaluate the pressure and temperature dependence of quartz solubility in H_2O up to ~10 kb, but solubility constraints at higher pressure are required to assess Si mass transfer by H_2O during fluid-rock interaction in, for example, subduction zones or magma source regions in the mantle. In addition, slow experimental quench times (8–10 min) may have led ANDERSON and BURNHAM (1965) to underestimate quartz solubilities at some conditions below 10 kb. Thus, accurate evaluation of the scale and magnitude of aqueous Si transport during fluid-rock interaction in mid-crustal to upper mantle environments requires new measurements of Si concentrations in H_2O in equilibrium with quartz at high pressures and temperatures.

Here, I present results of rapid-quench experiments on quartz solubility in H_2O at 500–900°C and 5–20 kb. The new determinations double the pressure range over which quartz solubility has been measured. Moreover, although quartz solubility is a complex function of solvent composition (e.g., SOMMERFIELD, 1967; SHETTEL, 1974; NOVGORODOV, 1975; HEMLEY et al., 1980; FOURNIER et al., 1982; WALTHER and ORVILLE, 1983; SACCOCIA and SEYFRIED, 1990; XIE and WALTHER, 1993), results in the simple system SiO_2–H_2O constrain the thermodynamic properties of aqueous silica needed for model phase equilibrium and transport calculations to upper-mantle pressures. This can be seen by writing the equilibrium between aqueous SiO_2 and quartz as

$$SiO_{2(quartz)} = SiO_{2(aq)}, \quad (1)$$

where $SiO_{2(aq)}$ refers to solvated aqueous silica independent of hydration state (WALTHER and HELGESON, 1977). Adopting standard states of unit activity (a) for pure quartz and H_2O at any pressure and temperature and unit activity for $SiO_{2(aq)}$ in a hypothetical one molal solution referenced to infinite dilution at any pressure and temperature, the mass-action relation for Eqn. 1 reduces to

$$\log K_{(1)} = \log a_{SiO_{2(aq)}}, \quad (2)$$

where $K_{(1)}$ is the equilibrium constant for equilibrium 1. WALTHER and HELGESON (1977) and WALTHER and ORVILLE (1983) noted that aqueous silica exists as a neutral hydrated monomer species in pure H_2O, so the activity coefficient of $SiO_{2(aq)}$ can be taken as unity, leading to

$$\log K_{(1)} = \log m_{SiO_{2(aq)}} \quad (3)$$

and

$$\Delta G^{\circ}_{SiO_{2(aq)}} = \Delta G^{\circ}_{quartz} - 2.303RT \log m_{SiO_{2(aq)}}, \quad (4)$$

where m is molality, ΔG° is the change in the apparent standard molal Gibbs free energy at constant pressure and temperature, R is the gas constant, and T is temperature in Kelvins. Thus, when combined with Eqns. 1–4 and appropriate derivatives, the new solubility measurements allow prediction of concentrations and thermodynamic properties of $SiO_{2(aq)}$ in pure H_2O over a wider range of conditions than has previously been possible: from the Earth's surface to its upper mantle.

EXPERIMENTAL METHODS

Two types of solubility experiments were conducted (Table 1). Initial experiments involved double encapsulation of crushed quartz grains following the methods of ANDERSON and BURNHAM (1965).

Table 1. Experimental results

Expt No.	T (°C)	P (kb)	Duration (hr)	Expt Type	w_{H_2O} (mg)	w^{i}_{qtz} (mg)	w^{f}_{qtz} (mg)	Solubility (wt %)	Solubility (mol/kg)	Notes
335	500	5	213.75	SC	63.684	7.412	6.911	0.781	0.131	
329	500	7.5	112.75	SC	67.272	7.952	7.356	0.878	0.147	
331	500	10	25.25	SC	63.688	19.945	19.291	1.016	0.171	
332	500	10	261.50	SC	73.952	9.452	8.684	1.028	0.173	
430	500	12.5	67.50	SC	74.712	11.071	10.265	1.067	0.180	
290	500	15	116.00	SC	69.480	8.124	7.221	1.283	0.216	from supersaturation
338	500	17.5	311.50	SC	67.521	9.175	8.242	1.363	0.230	
302	500	20	168.75	SC	61.674	11.527	10.676	1.361	0.230	
336	500	20	239.25	SC	72.942	8.767	7.772	1.346	0.227	
170	600	5	97.00	CQ	38.98	22.39	21.76	1.591	0.269	
431	600	5	92.00	SC	72.695	6.852	5.909	1.281	0.216	
432	600	5	85.50	SC	75.265	4.874	3.843	1.351	0.228	
312	600	7.5	96.50	SC	65.517	21.770	20.413	2.029	0.345	
287	600	10	43.75	SC	72.190	9.538	7.692	2.493	0.426	
311	600	10	137.75	SC	66.142	8.326	6.854	2.177	0.370	
344	600	10	119.50	SC	75.144	9.413	7.878	2.002	0.340	
327	600	12.5	63.50	SC	66.648	7.767	6.127	2.402	0.410	
343	600	12.5	122.50	SC	69.854	12.737	11.075	2.324	0.396	
307	600	15	232.00	SC	63.033	9.167	7.527	2.536	0.433	
308	600	17.5	92.00	SC	68.403	8.155	6.276	2.674	0.457	
309	600	20	89.25	SC	68.626	8.080	6.050	2.873	0.492	
236	615	7.5	53.00	SC	31.567	4.844	4.116	2.254	0.384	±15°C
250	615	10	92.00	SC	40.051	73.353	72.246	2.690	0.460	±15°C
238	615	12.5	95.00	SC	41.962	4.338	3.157	2.737	0.468	±15°C
241	615	15	48.50	SC	43.006	6.302	4.983	2.976	0.510	±15°C
247	615	17.5	68.00	SC	42.514	6.673	5.363	2.989	0.513	±15°C
145	700	5	64.50	CQ	36.36	28.21	27.27	2.520	0.430	
193	700	7	69.50	CQ	42.60	7.98	6.56	3.226	0.555	
95	700	8.8	47.00	CQ	26.70	10.63	9.60	3.714	0.642	perforated inner capsule
102	700	8.8	15.75	CQ	28.08	10.11	9.00	3.803	0.658	perforated inner capsule
105	700	8.8	24.50	CQ	28.43	8.83	7.70	3.823	0.662	perforated inner capsule
122	700	8.8	90.00	CQ	41.96	9.06	7.40	3.806	0.658	
128	700	8.8	67.00	CQ	40.24	19.42	17.84	3.778	0.654	
135	700	8.8	44.00	CQ	37.80	21.68	20.14	3.915	0.678	
136	700	8.8	71.00	CQ	42.49	20.73	19.25	3.366	0.580	20.5 min quench
139	700	8.8	43.50	CQ	34.02	26.00	24.77	3.489	0.602	10.0 min quench
142	700	8.8	43.00	CQ	36.10	24.30	22.98	3.528	0.609	4.4 min quench
143	700	8.8	67.50	CQ	39.01	23.93	22.47	3.608	0.623	2.7 min quench
147	700	12	42.00	CQ	37.07	25.01	23.32	4.360	0.759	
150	700	15	45.00	CQ	35.16	20.99	19.21	4.819	0.843	
283	700	17.5	42.00	SC	39.020	17.884	15.407	5.969	1.057	
175	800	5	47.00	CQ	38.24	19.29	17.76	3.847	0.666	
223	800	5	72.00	SC	37.522	7.072	5.581	3.822	0.661	
230	800	5	17.00	SC	49.635	4.546	2.593	3.786	0.655	
191	800	6.5	46.00	CQ	39.39	10.03	7.86	5.221	0.917	
178	800	7.5	36.00	CQ	39.20	16.51	14.10	5.792	1.023	
190	800	7.5	46.50	CQ	40.09	8.57	6.07	5.870	1.038	
231	800	10	21.00	SC	39.687	7.257	4.319	6.893	1.232	
181	900	8	20.00	CQ	39.55	12.39	8.16	9.662	1.780	
184	900	8	19.00	CQ	40.23	12.03	7.71	9.697	1.787	
187	900	9	46.00	CQ	44.89	11.21	5.45	11.372	2.136	
180	900	10	16.50	CQ	41.25	13.85	7.92	12.564	2.393	

Abbreviations: CQ, crushed-quartz experiments; SC, single-crystal experiments. Values of w_{H_2O} were corrected for solution trapped in inner capsule in CQ experiments. Unless noted, inner capsules were not perforated, quench times from experimental temperature to 100°C were ≤30 sec, and equilibrium was approached from undersaturation. Weighing precisions are ±1 in the last digit. Experiments at 615°C had large T uncertainty because thin-walled graphite furnaces led to T gradients; they were not used to derive eqn. 8.

These experiments are referred to as crushed-quartz experiments. Modifications of the capsule and furnace design (MANNING and BOETTCHER, 1994) allowed solubilities to be determined from single crystals. Experiments employing the new techniques are referred to as single-crystal experiments.

All experiments used inclusion-free Brazilian quartz. For crushed-quartz experiments, a large crystal was crushed and sieved. Grains from 0.35 to 0.42 mm in size were washed in H_2O in an ultrasonic bath and inspected for adhering ultrafines by optical and scanning-electron microscopy (Fig. 1a). In each crushed-quartz experiment, 20–40 μL distilled deionized H_2O and a crimped $Ag_{80}Pd_{20}$ 1.6 mm O.D. capsule with ~10 mg quartz were placed in 3 mm O.D. Pt capsules. The outer Pt capsule was then carefully crimped, weighed, sealed by arc welding, and weighed again. The replicate weighings identified water loss during each step. ANDERSON and BURNHAM (1965) used a perforated inner capsule. Exploratory experiments showed that this did not influence measured solubilities (Table 1), so inner capsules were left unperforated.

For single-crystal experiments, 3–4 mm thick slabs were cut normal to c from a large, subhedral crystal of the same Brazilian quartz used in the crushed-quartz experiments. Cylinders weighing 5–20 mg were drilled parallel to c with a 1.8 mm I.D. diamond coring bit (Fig. 1b). The microcores were cleaned with dilute HNO_3, placed in 2 mm O.D. Au capsules, and then loaded in a 5 mm O.D. Pt capsule together with 50–75 μL H_2O. Though not required for the measurement of solubility, the inner capsule prevented the microcore from breaking if it wedged into a corner of the outer capsule during an experiment.

An end-loaded piston-cylinder apparatus with 2.54 cm-diameter pistons and NaCl-graphite furnace assemblies was used for all experiments (BOHLEN, 1984; MANNING and BOETTCHER, 1994). Pressures were measured using Heise gauges calibrated against the melting of alkali halides (BOHLEN, 1984) and albite-jadeite-quartz equilibrium at 600°C (HAYS and BELL, 1973; MANNING and BOETTCHER, 1994). Pressure and temperature were held within 100 bars and 2°C of values listed in Table 1. All experiments employed Pt-$Pt_{90}Rh_{10}$ thermocouples resting on the capsules throughout the run. Capsules for crushed-quartz experiments were placed horizontally in the furnace assembly. For this geometry, the temperature gradients in the sample were ≤5°C (BOHLEN, 1984). Capsules used in single-crystal experiments had vertical lengths of 4–5 mm, but temperature gradients were similar to those in crushed-quartz experiments because thick graphite heaters with long hotspots were employed (MANNING and BOETTCHER, 1994). Since the magnitude of the effects of pressure, pressure gradients, and temperature gradients on emf are poorly known, uncorrected temperatures read from thermocouples are reported here. Note that following this standard convention likely introduces uncertainties of no more than 2.5–10°C at the conditions of the experiments (GETTING and KENNEDY, 1970; CHENG et al., 1975).

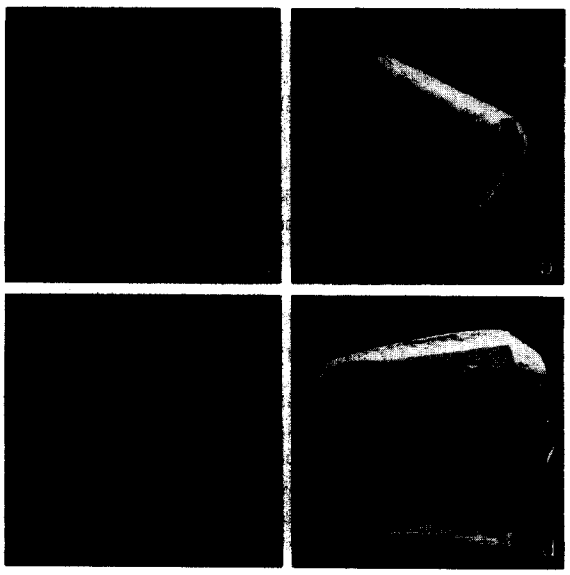

FIG. 1. Scanning electron micrographs of starting materials and experimental products. Scale bars are 60 μm. (a) and (b): starting materials for experiments using crushed quartz and single crystals, respectively. (c) and (d): products of crushed quartz (#95, 700°C, 8.8 kb) and single crystal experiments (#238, 615°C, 12.5 kb), respectively. The grain in (d) is 450 μm wide.

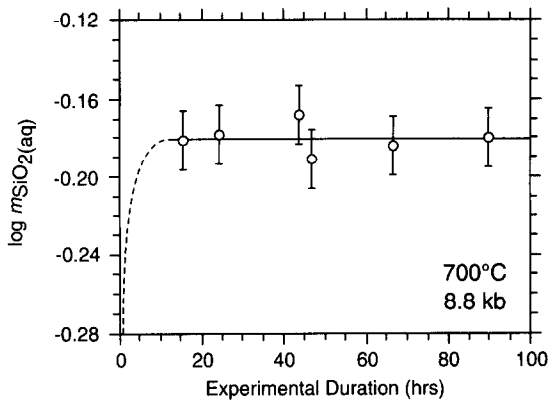

FIG. 2. Log m_{SiO_2} vs. experiment duration at 700°C and 8.8 kb. Solid line corresponds to the mean of the six experiments (log m_{SiO_2} = −0.181) and error bars are 2σ relative to mean (±0.016).

Experiments were quenched to <100°C in ≤30 s by cutting power to the apparatus. Pressure decreased to ~20–25% of run pressure during the temperature drop and was then lowered to 1 atm over several minutes. Total time from quench to quartz weighing was, typically, ~15 min. Final aqueous solutions ranged from clear to milky, evidently depending on the degree of formation of colloidal silica on quench. Dried material from fluid in the outer capsule was isotropic and had an index of refraction <1.52, consistent with vapor quench. Occasionally, up to three or four small quartz crystals could be found in this material. It is unclear whether they sifted out from the inner capsule or precipitated on quench, but their weight was undetectable and thus, too small to affect solubility determinations.

Quartz from the inner capsule was carefully inspected for adhering quench material using optical and scanning-electron microscopy. In crushed-quartz experiments (Fig. 1c), the crystals showed subhedral terminations and a wider range in grain size than the starting material, suggesting substantial dissolution and reprecipitation during the experiments. This is consistent with an abundance of two-phase fluid inclusions in the product grains. In single-crystal experiments, optical inspection readily revealed any adhering particles or signs of breakage. In some cases, well-developed growth facets formed at one or both ends of the cylinder (Fig. 1d).

Quartz solubility was determined from the weight loss of quartz grains by

$$m_{SiO_{2(aq)}} = \frac{(w^i_{qtz} - w^f_{qtz}) \times 1000}{60.048 w_{H_2O}}, \quad (5)$$

where w^i_{qtz} and w^f_{qtz} are the initial and final weights of quartz, the number 60.048 is the molecular weight of SiO_2, and w_{H_2O} is the weight of H_2O in the experiment. ANDERSON and BURNHAM (1965) noted that SiO_2 precipitates from the solution trapped in the inner capsule in crushed-quartz experiments. This problem was eliminated by subtracting from w_{H_2O} the weight of the trapped solution as measured by the difference between wet and dry weighings. Trapped solution averaged 5 wt% of the fluid.

Run durations required for equilibration were assessed at 700°C. Measured solubilities for experiments lasting from 15.75 to 90 h do not vary with time (Fig. 2). Accordingly, all experiments at ≥700°C were ≥16 h in duration. ANDERSON and BURNHAM (1965) reported that 50 to 60 h were required for equilibrium at 500°C. These were taken as minimum durations for experiments at 500 and 600°C.

WALTHER and ORVILLE (1983) showed that, at low pressures, experiments approaching equilibrium from both undersaturation and supersaturation gave results consistent with previous experiments in which equilibrium was approached from undersaturation. In this study, all but one of the experiments approached equilibrium from undersaturation.

RESULTS

Table 1 and Fig. 3 give experimentally determined quartz solubilities in H_2O along isotherms between 500 and 900°C. The same type of apparatus was used for all experiments and all solubilities were determined by weight loss, so it can be assumed that sources of random error are similar for all measurements. Uncertainties can therefore be established by pooling repeated experiments through the equation

$$\sigma = \sqrt{\frac{\sum_{i=1}^{N_1} (m_i - \bar{m}_1)^2 + \sum_{j=1}^{N_2} (m_j - \bar{m}_2)^2 + \cdots}{N_1 + N_2 + \cdots + N_s}} \quad (6)$$

(e.g., SKOOG et al., 1994), where σ is the sample standard deviation, m_n is the nth solubility measurement at a given P and T, and $\bar{m}_1$ and N_1 are the mean measured solubility and number of experiments at the first P and T, $\bar{m}_2$ and N_2 are the mean measured solubility and number of experiments at the second P and T, and so on for N_s distinct experimental conditions. Nine sets of two to six replicates (Table 1) yield a pooled sample standard deviation of 0.020 molal. Uncertainty levels in Fig. 3 are two standard deviations. Note that the level of uncertainty for the dataset as a whole is greater than that inferred for 700°C and 8.8 kb (Fig. 2), because fewer repeat experiments were carried out at other pressures and temperatures (Table 1).

Figure 3 shows that the solubility of quartz in H_2O increases with increasing pressure along each isotherm. When compared with the results of ANDERSON and BURNHAM (1965), the present study illustrates that $(\partial \log m_{SiO_{2(aq)}}/\partial P)_T$ is greatest below 5 kb and decreases strongly with increasing pressure. The results also confirm that, at constant pressure, quartz solubility increases with temperature at high pressures.

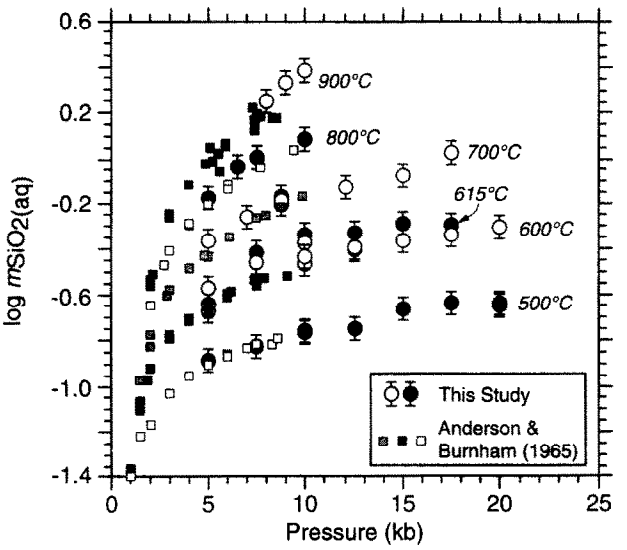

FIG. 3. Experimental results as a function of pressure. Uncertainties are 2σ from pooled replicate experiments (see text). Results of ANDERSON and BURNHAM (1965) are shown for comparison. Fill patterns vary to allow distinction of isothermal datasets.

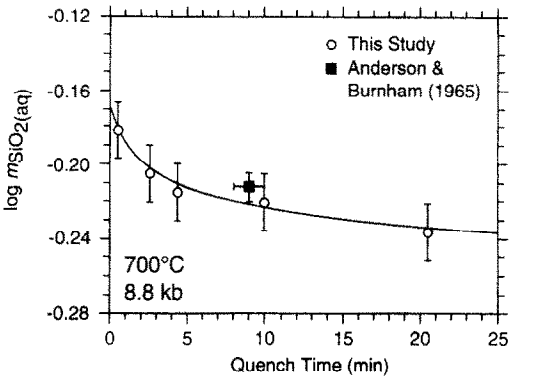

FIG. 4. Dependence of log m_{SiO_2} on quench time at 700°C, 8.8 kb. Shown are results of this study and of ANDERSON and BURNHAM (1965). Uncertainties for results of this study as in Fig. 2.

The solubilities reported by ANDERSON and BURNHAM (1965) are similar to those measured here at 500°C, but their results are systematically near the lower limit of my 2σ uncertainties at ≥600°C (Fig. 3). The most likely explanation is the different quench times used in each study. ANDERSON and BURNHAM (1965) used a gas apparatus and reported quench times of 8–10 min from the experimental temperature to <100°C. Similar temperature drops required ≤30 s in the piston-cylinder apparatus used here. I investigated the effect of these different quench times at 700°C and 8.8 kb. After sufficient time for equilibration, temperatures were decreased linearly to 100°C over 0.5 to ~20 min. Figure 4 illustrates that apparent solubility increases with decreasing quench times. Because apparent solubility decreases most strongly between 0 and 2 min quench times (Fig. 4), rapid quenching is required for accurate solubility determinations where concentrations are high. Aware of this problem, ANDERSON and BURNHAM (1965) attributed decreasing precision at high solubility (Fig. 3) to reprecipitation of quartz on quench. Figures 3 and 4 imply that their solubilities may be too low by up to 10% at ≥600°C.

DISCUSSION

Equation for Quartz Solubility to High Pressures

Though accurate for most mid- to upper-crustal conditions, previous equations for computing the solubility of quartz in pure H_2O can not be used at the higher pressures of the present study. WALTHER and HELGESON (1977) predicted quartz solubilities to 550°C and 5 kb. MCKENZIE and HELGESON (1984) extended these results to 900°C at 2 kb. Subsequent modifications to the Helgeson-Kirkham-Flowers (HKF; HELGESON et al., 1981) equation of state for aqueous species (TANGER and HELGESON, 1988) allowed SHOCK et al. (1989) to improve and extend the predicted thermodynamic properties of $SiO_{2(aq)}$ to 1000°C at ≤5 kb. The HKF model has the advantage that its parameters describe specific solvation

and nonsolvation contributions to thermodynamic properties of aqueous species. However, the solvation contributions depend in part on the static dielectric constant of H_2O (ϵ_{H_2O}) and its derivatives. Despite apparently reliable estimates of ϵ_{H_2O} at water densities below 1.0 g/cm^3 (e.g., PITZER, 1983; WALTHER, 1991), the lack of experimental data or adequate predictive models for ϵ_{H_2O} at higher densities currently limit use of the HKF model to ≤5 kb. FOURNIER and POTTER (1982) described quartz solubility to 10 kb using a correlation equation based on temperature and the specific volume of H_2O, for which experimental data exist within the fit range. However, their equation is strongly weighted by the data of ANDERSON and BURNHAM (1965). Moreover, extrapolations beyond ~10 kb do not reproduce the solubilities measured in the present study.

At constant temperature, values of log K for the ionization of H_2O and a variety of other aqueous species are linear in the logarithm of the density (ρ) of H_2O over a range in pressure (FRANCK, 1956, 1961; QUIST, 1970; MARSHALL and QUIST, 1967; MARSHALL, 1970, 1972; SWEETON et al., 1974; MARSHALL and FRANCK, 1981; MARSHALL and MESMER, 1984; MESMER et al., 1988, 1989). As noted by WALTHER (1991), this linear behavior is probably a consequence of the linear correlations between temperature and $1/\epsilon_{H_2O}$ at constant water density. MARSHALL and FRANCK (1981) showed that the ionization of H_2O to 1000°C and 10 kb could be parameterized by an equation of the form

$$\log K = A + \frac{B}{T} + \frac{C}{T^2} + \frac{D}{T^3} + \left[E + \frac{F}{T} + \frac{G}{T^2}\right] \log \rho_{H_2O}, \quad (7)$$

where the terms A through G are regressed constants. This equation has two parts: a third-order polynomial fit to $(\partial \log K/\partial(1/T))$ at ρ_{H_2O} = 1.0 g/cm^3 (terms A–D), and a second-order polynomial fit to $(\partial \log K/\partial \log \rho_{H_2O})_T$ vs. $1/T$ (terms E–G). Equation 7, or variants, have been explored for geologic conditions by EUGSTER and BAUMGARTNER (1987) and ANDERSON et al. (1991). Its dependence only on temperature and ρ_{H_2O} makes Eqn. 7 ideal for calculating thermodynamic properties of aqueous species at high pressures, provided that ρ_{H_2O} is known and that linear dependence of log K on log ρ_{H_2O} can be demonstrated.

Use of Eqn. 7 to predict quartz solubilities from the surface of the Earth to the upper mantle requires accurate calculation of the density of H_2O from 1 bar to >100 kb and 25 to ≥1000°C, such that density is a continuous function of temperature and pressure. Many equations of state and molecular-dynamics simulations compute the thermodynamic properties of H_2O for different geologic conditions (RICE and WALSH, 1957; HELGESON and KIRKHAM, 1974; HOLLOWAY, 1977; DELANY and HELGESON, 1978; KERRICK and JACOBS, 1981; HALBACH and CHATTERJEE, 1982; HAAR et al., 1984; SAXENA and FEI, 1987a,b; SAUL and WAGNER, 1989; BRODHOLDT and WOOD, 1990; HILL, 1990; STIXRUDE and BUKOWINSKI, 1990; BELONOSHKO and SAXENA, 1991; HOLLAND and POWELL, 1991). But, as noted by HOLLAND and POWELL (1991), most available equations are not applicable over the wide pressure-temperature range desired. Exceptions are the equations of HALBACH and CHATTERJEE (1982), SAUL and WAGNER (1989), and HOLLAND and POWELL (1991). The empirical Redlich-Kwong formulation of HALBACH and CHATTERJEE (1982) was used in the present study to calculate ρ_{H_2O} because it accurately represents the properties of water to 50 kb and 1000°C (e.g., RICE and WALSH, 1957; BULAKH, 1979), it can be extrapolated to higher pressures, and it is simple in form.

The many investigations of the solubility of quartz in H_2O provide a set of experimental constraints that range widely not only in pressure and temperature, but also in accuracy and precision. Nevertheless, as illustrated in Fig. 5, the variation in log $m_{SiO_{2(aq)}}$ with log ρ_{H_2O} (HALBACH and CHATTERJEE, 1982) along isotherms from selected experiments is remarkably linear. Previous studies also noted this behavior over more limited density intervals (e.g., MOSEBACH, 1957). Although FOURNIER and POTTER (1982) suggested that isotherms become nonlinear at high temperatures below the critical density (ρ_{H_2O} < 0.322 g/cm^3), Fig. 5 implies that the assumption of linear behavior for most geologic conditions is justified.

In the regression analysis, I combined the new measurements with the results of HEMLEY et al. (1980) and WALTHER and ORVILLE (1983) to ensure that experiments of both high and low quality were not averaged. These studies were used for two reasons. First, they avoided quench problems through rapid quenching (HEMLEY et al., 1980) or solution extraction at pressure and temperature (WALTHER and ORVILLE, 1983). Also, the two studies could be combined to generate isothermal solubility measurements from the boiling curve of H_2O to 2 kb at 200–550°C needed for the fit procedure. To constrain Eqn. 7 below 200°C, solubilities were calculated to 5 kb along isotherms of 25, 50, 100, and 150°C from FOURNIER and POTTER (1982).

Regression of the experimental data gave

$$\log K_{(1)} = 4.2620 - \frac{5764.2}{T} + \frac{1.7513 \times 10^6}{T^2} - \frac{2.2869 \times 10^8}{T^3} + \left[2.8454 - \frac{1006.9}{T} + \frac{3.5689 \times 10^5}{T^2}\right] \log \rho_{H_2O}. \quad (8)$$

The correlation coefficient (R) for the polynomial describing the variation in log $K_{(1)}$ with $1/T$ at ρ_{H_2O} = 1.0 gm/cm^3 is 0.9989. A lower value of R = 0.6942 was obtained for the fit to $(\partial \log K/\partial \log \rho_{H_2O})_T$ as a function of $1/T$. This is because of fewer data from HEMLEY et al. (1980) and WALTHER and ORVILLE (1983) along some isotherms, which results in lower precision of calculated changes in the slopes of isotherms with temperature. However, the low R does not appear to affect significantly the accuracy of predicted solubilities.

Comparison to Previous Work

Figure 5 compares calculated solubilities (Eqn. 8) with selected experiments. It is evident in Fig. 5 that there are no systematic deviations between calculated solubilities and those experiments used in the derivation of Eqn. 8. Also, predicted solubilities are somewhat greater than those of ANDERSON and BURNHAM (1965), consistent with the inference of minor reprecipitation on quench in their experiments.

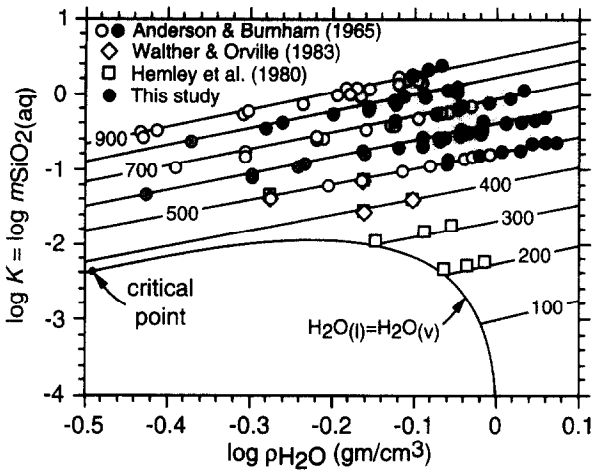

FIG. 5. Log m_{SiO_2} vs. log ρ_{H_2O} for selected experimental studies (ANDERSON and BURNHAM, 1965; HEMLEY et al., 1980; WALTHER and ORVILLE, 1983; this study). Symbol sizes greater than or equal to reported uncertainties. Solid lines are values of log $m_{SiO_{(aq)}}$ calculated from Eqn. 8, labeled in °C.

Equation 8 predicts that log $K_{(1)} = -4.003$ at 25°C and 1 bar. This agrees well with the values of −4.001 of MOREY et al. (1962) and −3.992 of SUPCRT92 (JOHNSON et al., 1992). The degree to which Eqn. 8 reproduces other experimental data at elevated pressures and temperatures can be assessed using average differences, $\bar{\Delta}$, between experimental and calculated solubilities, where $\Delta = \log m_{experimental} - \log m_{calculated}$. The sign of $\bar{\Delta}$ signifies whether, on average, calculated solubilities underestimate (positive $\bar{\Delta}$) or overestimate (negative $\bar{\Delta}$) those measured; the average of the absolute values of Δ, $|\bar{\Delta}|$, is a measure of the precision of the calculated values with respect to the experimental values. Table 2 compares values of $\bar{\Delta}$ and $|\bar{\Delta}|$ generated using equations of FOURNIER and POTTER (1982), the data of SHOCK et al. (1989) in SUPCRT92 (JOHNSON et al., 1993), and Eqn. 8. Calculations were confined to experiments within the stated pressure and temperature limits of each study: ≤5 kb in the case of SHOCK et al. (1989) and ≤10kb in the case of FOURNIER and POTTER (1982). Values in Table 2 differ slightly from those given by FOURNIER and POTTER (1982), because of different equations of state for H_2O. The similar magnitudes of $|\bar{\Delta}|$ for all three studies imply a similar level of precision for each. Values of $\bar{\Delta}$ vary somewhat between the three studies, indicating that predicted quartz solubilities are optimized at different pressures and temperatures. There is good agreement between Eqn. 8 and the results of KENNEDY (1950), MOREY and HESSELGESSER (1951), WYART and SABATIER (1955), WEILL and FYFE (1964), and CRERAR and ANDERSON (1971). Solubilities measured by KHITAROV (1956), KITAHARA (1960), and ANDERSON and BURNHAM (1965) are systematically low relative to Eqn. 8, probably because of quench problems. VAN LIER et al. (1960), MOREY et al. (1962), and SIEVER (1962) measured higher solubilities than those predicted by Eqn. 8. FOURNIER and POTTER (1982), who also underestimated these solubilities, suggested that the higher surface energies of finely ground quartz used in these experiments caused fluid supersaturation with respect to quartz. The results of RIMSTIDT (1984) are also greater than those predicted by Eqn. 8, as well as by FOURNIER and POTTER (1982) and SHOCK et al. (1989). Because ultrafine problems were carefully avoided, it is unclear why his results are inconsistent with all three equations for quartz solubility.

Figure 6 illustrates graphically the success of Eqn. 8 in predicting quartz solubilities from liquid-vapor saturation to 2 kb over a range in temperatures. With the exception of the data of HEMLEY et al. (1980) and WALTHER and ORVILLE (1983), none of the additional ~200 solubility determinations by other workers were used to derive Eqn. 8. Of particular note is the sharp predicted decrease in quartz solubility within several °C of the critical point (Fig. 6a), a feature that has previously proved difficult to reproduce (e.g., WALTHER and HELGESON, 1977; SHOCK et al., 1989).

Table 2. Comparison of calculated and measured quartz solubilities in H_2O

	P range (kb)	T range (°C)	Fournier & Potter (1982) $\bar{\Delta}$*	Fournier & Potter (1982) $\lvert\bar{\Delta}\rvert$**	Shock et al. (1989) $\bar{\Delta}$	Shock et al. (1989) $\lvert\bar{\Delta}\rvert$	This Study $\bar{\Delta}$	This Study $\lvert\bar{\Delta}\rvert$
Used to derive eq. (8)								
This Study	5-20	500-900	-	-	-	-	-0.031	0.035
Hemley et al. (1980)	P_{sat}-2	200-500	-0.010	0.031	0.033	0.040	-0.031	0.043
Walther & Orville (1983)	1-2	350-550	-0.011	0.013	0.014	0.022	-0.012	0.036
Independent of eq. (8)								
Anderson & Burnham (1965)	1-9	500-900	-0.033	0.042	-0.012	0.029	-0.059	0.059
Crerar & Anderson (1971)	P_{sat}	179-329	-0.051	0.054	0.013	0.034	-0.006	0.023
Kennedy (1950)	P_{sat}-1.75	160-610	-0.059	0.069	0.005	0.066	-0.038	0.070
Khitarov (1956)	1.5-4	400	-0.038	0.038	-0.057	0.057	-0.026	0.026
Kitahara (1960)†	P_{sat}	140-370	-0.095	0.102	-0.060	0.127	-0.057	0.098
Morey & Hesselgesser (1951)	0.3-2	300-600	-0.017	0.085	0.033	0.086	-0.006	0.072
Morey et al. (1962)	1	25-300	0.057	0.077	0.032	0.054	0.062	0.083
Rimstidt (1984)	P_{sat}	50-96	0.126	0.126	0.092	0.092	0.080	0.080
Siever (1962)	P_{sat}	125-182	0.094	0.094	0.110	0.110	0.084	0.084
Van Lier et al. (1960)	P_{sat}	70-100	0.158	0.158	0.121	0.201	0.107	0.107
Weill & Fyfe (1964)	1-4	400-550	-0.005	0.013	0.029	0.051	-0.015	0.020
Wyart & Sabatier (1955)	0.5-2	400	-0.051	0.051	-0.017	0.019	-0.037	0.037

* $\bar{\Delta}$ = average difference between experimental and calculated log $m_{SiO_{2(aq)}}$ (see text).

** $|\bar{\Delta}|$ = average of the absolute value of the difference between experimental and calculated log $m_{SiO_{2(aq)}}$ (see text).

† P_{sat} data only (see FOURNIER and POTTER, 1982).

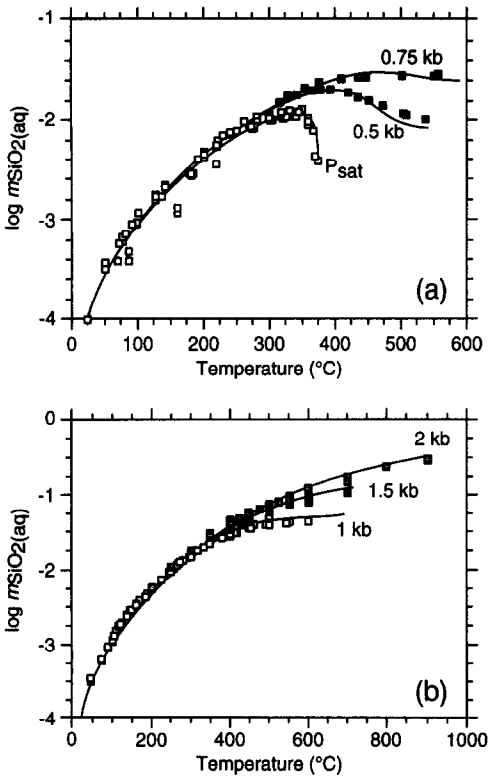

FIG. 6. (a and b) Log m_{SiO_2} vs. temperature along steam saturation curve and selected isobars. Published experimental solubility determinations shown in squares (KENNEDY, 1950; MOREY and HESSELGESSER, 1951; WYART and SABATIER, 1955; KITAHARA, 1960; VAN LIER et al., 1960; MOREY et al., 1962; SIEVER, 1962; WEILL and FYFE, 1964; ANDERSON and BURNAHM, 1965; CRERAR and ANDERSON, 1971; HEMLEY et al., 1980; WALTHER and ORVILLE, 1983; RIMSTIDT, 1984). Solid curves predicted from Eqn. 8.

The System SiO_2-H_2O to High Pressures

The observation that log $K_{(1)}$ is linear with respect to log ρ_{H_2O} to 20 kb provides the basis for extrapolation of the results beyond 20 kb. At constant temperature, log ρ_{H_2O} increases only slightly with increasing pressure at high pressures. Thus, application of Eqn. 8 to higher pressures probably will not lead to substantial errors in predicted log $K_{(1)}$, even if future experiments demonstrate that it is not linear in log ρ_{H_2O} above 20 kb.

Figure 7 shows phase relations in the system SiO_2-H_2O assuming saturation with respect to the stable SiO_2 polymorph and linear extrapolation of log $K_{(1)}$ with log ρ_{H_2O} above 20 kb. Polymorphic transformations of SiO_2 are superimposed on the diagram from data of BERMAN (1988), MIRWALD and MASSONE (1980), and BOHLEN and BOETTCHER (1982). Values of log $m_{SiO_{2(aq)}}$ along the H_2O-saturated melting curve of SiO_2 are from KENNEDY et al. (1962), whereas those in equilibrium with H_2O ices were derived from Eqn. 8, using ρ_{H_2O} calculated along the stable phase boundaries reported by BRIDGMAN (1937) and PISTORIUS et al. (1963). Figure 7 illustrates phase relations from 25°C to water-saturated melting and from 1 bar to >50 kb. As noted above, log $K_{(1)}$ varies linearly with log ρ_{H_2O} along isotherms. In contrast, isobaric variation in log $K_{(1)}$ is not linear. Log $K_{(1)}$ increases with temperature along low-pressure isobars (<1 kb) to a maximum between 300 and 350°C and then decreases, producing the well-known "reverse-solubility" behavior of quartz (Fig. 6a). At higher pressures, log $K_{(1)}$ increases with temperature at constant pressure and $(\partial \log K_{(1)}/\partial \log \rho_{H_2O})_P$ decreases. Also, Fig. 7 shows that $(\partial^2 \log K_{(1)}/\partial(\log \rho_{H_2O})^2)_P$ decreases significantly with increasing pressure.

Combining Eqns. 4 and 8 with $\Delta G^\circ_{\text{cocsite}}$ (BERMAN, 1988) allows prediction of the solubility of coesite in H_2O. Figure 7 illustrates that log $m_{SiO_{2(aq)}}$ in H_2O in equilibrium with coesite decreases with increasing water density below ~800°C.

KENNEDY et al. (1962) determined a critical endpoint in the system SiO_2–H_2O at 1080°C and 9.7 kb. Because this defines complete miscibility in the system, log $m_{SiO_{2(aq)}}$ should approach infinity at this pressure and temperature. Thus, the slopes of isotherms should approach infinity near the temperature of the endpoint. Although calculated slopes of isotherms increase slightly above 500°C (Fig. 7) and are accurate

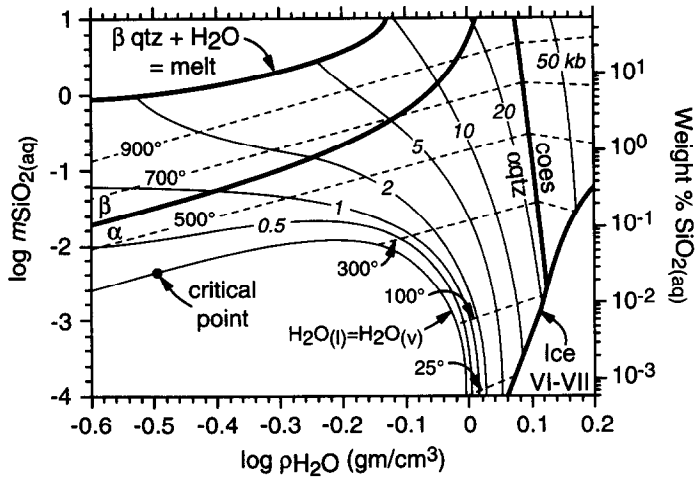

FIG. 7. Phase diagram for the system SiO_2–H_2O showing wt% SiO_2 and log m_{SiO_2} in H_2O in equilibrium with the stable SiO_2 polymorph at any given pressure and temperature. Phase boundaries (heavy lines) superimposed on diagram from BRIDGMAN (1937), KENNEDY et al. (1962), PISTORIUS et al., (1963), and BERMAN (1988). Light dashed and solid curves are respectively isotherms and isobars calculated from Eqn. 8.

at the temperatures and pressures investigated experimentally, Eqn. 8 does not reproduce this critical behavior. Experiments on quartz solubility at pressures and temperatures near the critical endpoint would allow refinement of Eqn. 8 to account for the results of KENNEDY et al. (1962).

Figure 7 provides a basis for comparing aqueous SiO_2 concentrations from different geologic environments. For example, the formation of eclogite from hydrous metabasaltic assemblages in subduction zones liberates water that may play an important role in metasomatism and melt generation in the mantle wedge. These reactions proceed at or near quartz saturation over a range in pressure and temperature of ~12–15 kb and 500–600°C (e.g., PEACOCK, 1993). Figure 7 shows that log $m_{SiO_{2(aq)}}$ in aqueous pore fluids in equilibrium with quartz at these conditions is ~0.7 to −0.2, or 0.3 to 0.6 mol/kg. By comparison, peak metamorphic conditions in Barrovian metamorphic belts may reach 600–700°C and 6–8 kb. Si concentrations in aqueous pore fluids in equilibrium with quartz in this environment would be 0.4–0.6 mol/kg (Fig. 7). The capacity for silica transport in and above subducting oceanic crust is therefore broadly similar to that in the deeper portions of orogenic belts, assuming pure H_2O. Thus, use of Fig. 7 and Eqn. 8 allows simple comparisons such as these for a wide range of geologic settings, as well as more detailed analyses of Si mass transfer in previously inaccessible metasomatic environments. Moreover, the single equation describing log $K_{(1)}$ over a wide range of pressures and temperatures ensures internal consistency for comparing Si metasomatism between environments or along pressure-temperature paths.

CONCLUSIONS

New experiments on the solubility of quartz in H_2O provide the first systematic data on the thermodynamic properties of $SiO_{2(aq)}$ between 10 and 20 kb. Because of the rapid-quench methods used, the results also lead to more accurate estimation of quartz solubilities at lower pressures. By combining these experiments with previous high-quality results, a simple equation correlating quartz solubility with the density of H_2O allows calculation of the concentrations of SiO_2 in aqueous fluids from the surface of the Earth to the upper mantle. These results can be used to model Si metasomatism in magma-source regions in the mantle, in subducting slabs and the overlying mantle wedge, and in Barrovian metamorphic belts.

Acknowledgments—This study was supported by NSF EAR 9104288 and 9205956. I thank J. Walther and I.-M. Chou for helpful reviews, and S. Boettcher and S. Bohlen for experimental assistance and advice. K. Knesel, H. Lin, and D. Rothstein read and improved an early draft of the manuscript.

Editorial handling: R. C. Burruss

REFERENCES

ANDERSON G. M. and BURNHAM C. W. (1965) The solubility of quartz in supercritical water. *Amer. J. Sci.* **263**, 494–511.

ANDERSON G. M. and BURNHAM C. W. (1967) Reactions of quartz and corundum with aqueous chloride and hydroxide solutions at high temperatures and pressures. *Amer. J. Sci.* **265**, 12–27.

ANDERSON G. M., CASTET S., SCHOTT J., and MESMER R. E. (1991) The density model for estimation of thermodynamic parameters of reactions at high temperatures and pressures. *Geochim. Cosmochim. Acta* **55**, 1769–1779.

BELONOSHKO A. and SAXENA S. K. (1991) A molecular dynamics study of the pressure-volume-temperature properties of supercritical fluids: I. H_2O. *Geochim. Cosmochim. Acta* **55**, 381–388.

BERMAN R. G. (1988) Internally-consistent thermodynamic data for minerals in the system Na_2O–K_2O–CaO–MgO–FeO–Fe_2O_3–Al_2O_3–SiO_2–TiO_2–H_2O–CO_2. *J. Petrol.* **29**, 445–522.

BOHLEN S. R. (1984) Equilibria for precise pressure calibration and a frictionless furnace assembly for the piston-cylinder apparatus. *Neues Jb. Mineral. Mh.* **9**, 404–412.

BOHLEN S. R. and BOETTCHER A. L. (1982) The quartz-coesite transformation: A precise determination and the effects of other components. *J. Geophys. Res.* **87**, 7073–7078.

BRIDGMAN P. W. (1937) The phase diagram of water to 45,000 kg/cm^2. *J. Chem. Phys.* **5**, 964–966.

BRODHOLT J. and WOOD B. J. (1990) Molecular dynamics of water at high temperatures and pressures. *Geochim. Cosmochim. Acta.* **54**, 2611–2616.

BULAKH A. G. (1979) Thermodynamic properties and phase transitions of H_2O up to 1000°C and 100 kbar. *Int. Geol. Rev.* **21**, 92–103.

CHENG V. M., ALLEN P. C., and LAZARUS D. (1975) Pressure coefficient of thermoelectric power of platinum/platinum-10% rhodium and chromel/alumel thermocouples. *Appl. Phys. Lett.* **26**, 6–7.

CRERAR D. A. and ANDERSON G. M. (1971) Solubility and solvation reactions of quartz in dilute hydrothermal solutions. *Chem. Geol.* **8**, 107–122.

DELANY J. M. and HELGESON H. C. (1978) Calculation of the thermodynamic consequences of dehydration in subducting oceanic crust to 100 kb and >800°C. *Amer. J. Sci.* **278**, 638–686.

EUGSTER H. P. and BAUMGARTNER L. P. (1987) Mineral solubilities and speciation in supercritical metamorphic fluids. In *Thermodynamic Modeling of Geological Materials: Minerals, Fluids and Melts* (ed. I. S. E. CARMICHAEL and H. P. EUGSTER); *Rev. Mineral.* **17**, 367–403.

FOURNIER R. O. and POTTER R. W., II (1982) An equation correlating the solubility of quartz in water from 25 to 900°C at pressures up to 10,000 bars. *Geochim. Cosmochim. Acta* **46**, 1969–1973.

FOURNIER R. O., ROSENBAUER R. J., and BISCHOFF J. L. (1982) The solubility of quartz in aqueous sodium chloride solutions at 350°C and 180 to 500 bars. *Geochim. Cosmochim. Acta* **46**, 1969–1978.

FRANCK E. U. (1956) Hochverdichteter Wasserdampf II. Ionendissociation von KCl in H_2O bis 750°C. *Z. Phys. Chem.* **8**, 107–126.

FRANCK E. U. (1961) Überkritisches Wasser als electrolytisches Lösungsmittel. *Angew. Chem.* **73**, 309–322.

GETTING I. C. and KENNEDY G. C. (1970) Effect of pressure on the emf of chromel-alumel and platinum-platinum 10% rhodium thermocouples. *J. Appl. Phys.* **41**, 4552–4562.

HAAR L., GALLAGHER J. S., and KELL G. S. (1984) *NBS/NRC Steam Tables*. Hemisphere.

HALBACH H. and CHATTERJEE N. D. (1982) An empirical Redlich-Kwong-type equation of state for water to 1000°C and 200 kbar. *Contrib. Mineral. Petrol.* **79**, 337–345.

HAYS J. F. and BELL P. M. (1973) Albite-jadeite-quartz equilibrium: a hydrothermal static determination. *Eos.* **54**, 482.

HEITMANN H.-G. (1965) Die Löslichkeit von Kieselsäure in Wasser und Wasserdampf. *Glastech. Ber.* **38**, 41–54.

HELGESON H. C. and KIRKHAM D. H. (1974) Theoretical prediction of the thermodynamic behavior of aqueous electrolytes at high pressures and temperatures. I. Summary of the thermodynamic/electrostatic properties of the solvent. *Amer. J. Sci.* **274**, 1089–1198.

HELGESON H. C., KIRKHAM D. H., and FLOWERS G. C. (1981) Theoretical prediction of the thermodynamic behavior of aqueous electrolytes at high pressures and temperatures: IV. Calculation of activity coefficients, osmotic coefficients, and apparent molal and standard and relative partial molal properties to 600°C and 5 kb. *Amer. J. Sci.* **281**, 1249–1516.

HEMLEY J. J., MONTOYA J. W., MARINENKO J. W., and LUCE R. W. (1980) Equilibria in the system Al_2O_3–SiO_2–H_2O and some general implications for alteration/mineralization processes. *Econ. Geol.* **75**, 210–228.

HILL P. G. (1990) A unified fundamental equation for the thermodynamic properties of H_2O. *J. Phys. Chem. Ref. Data* **19**, 1233–1274.

HOLLAND T. J. B. and POWELL R. (1991) A compensated-Redlich-Kwong (CORK) equation for volumes and fugacities of CO_2 and H_2O in the range 1 bar to 50 kbar and 100–1600°C. *Contrib. Mineral. Petrol.* **109,** 265–273.

HOLLOWAY J. R. (1977) Fugacity and activity of molecular species in supercritical fluids. In *Thermodynamics in Geology* (ed. D. G. FRASER), pp. 161–181. Reidel.

JOHNSON J. W., OELKERS E. H., and HELGESON H. C. (1992) SUPCRT92: A software package for calculating the standard molal thermodynamic properties of minerals, gases, aqueous species, and reactions from 1 to 5000 bar and 0° to 1000°C. *Comp. Geosci.* **18,** 899–947.

KENNEDY G. C. (1950) A portion of the system silica-water. *Econ. Geol.* **45,** 629–653.

KENNEDY G. C., WASSERBURG G. J., HEARD H. C., and NEWTON R. C. (1962) The upper three-phase region in the system SiO_2–H_2O. *Amer. J. Sci.* **260,** 501–521.

KERRICK D. M. and JACOBS G. K. (1981) A modified Redlich-Kwong equation for H_2O, CO_2, and H_2O-CO_2 mixtures at elevated pressures and temperatures. *Amer. J. Sci.* **281,** 735–767.

KHITAROV N. I. (1956) The 400°C isotherm for the system H_2O–SiO_2 at pressures up to 2,000 kg/cm^2. *Geochemistry* **1956,** 55–61.

KITAHARA S. (1960) The solubility of quartz in water at high temperatures and high pressures. *Rev. Phys. Chem. Japan* **30,** 109–114.

MANNING C. E. and BOETTCHER (1994) Rapid-quench hydrothermal experiments at mantle pressures and temperatures. *Amer. Mineral.* **79,** 1153–1158.

MARSHALL W. L. (1970) Complete equilibrium constants, electrolyte equilibria, and reaction rates. *J. Phys. Chem.* **74,** 346–355.

MARSHALL W. L. (1972) A further description of complete equilibrium constants. *J. Phys. Chem.* **76,** 720–731.

MARSHALL W. L. and FRANCK E. U. (1981) Ion product of water substance, 0–1000°C, 1–10,000 bars, new international formulation and its background. *J. Phys. Chem. Ref. Data* **10,** 295–304.

MARSHALL W. L. and MESMER R. E. (1984) Pressure-density relationships and ionization equilibria in aqueous solutions. *J. Soln. Chem.* **13,** 383–391.

MARSHALL W. L. and QUIST A. S. (1967) A representation of isothermal ion-ion-pair solvent equilibria independent of changes in dielectric constant. *Nat. Acad. Sci. Proc.* **58,** 901–906.

MCKENZIE W. F. and HELGESON H. C. (1984) Estimation of the dielectric constant of H_2O from experimental solubilities of quartz and calculation of the thermodynamic properties of aqueous species to 900°C at 2 kb. *Geochim. Cosmochim. Acta* **48,** 2167–2177.

MESMER R. E., MARSHALL, W. L., PALMER D. A., SIMONSON J. M., and HOLMES H. F. (1988) Thermodynamics of aqueous association and ionization reactions at high temperatures and pressures. *J. Soln. Chem.* **17,** 699–718.

MESMER R. E., PATTERSON C. S., BUSEY R. H., and HOLMES H. F. (1989) Ionization of acetic acid in NaCl(aq) media: A potentiometric study to 573 K and 130 bar. *J. Phys. Chem.* **93,** 7483–7490.

MIRWALD P. W. and MASSONE H.-J. (1980) The low-high quartz and quartz-coesite transition to 40 kbar between 600° and 1600°C and some reconnaissance data on the effect of $NaAlO_2$ component on the low quartz-coesite transition. *J. Geophys. Res.* **85,** 6983–6990.

MOREY G. W. and HESSELGESSER J. M. (1951) The solubility of some minerals in superheated steam at high pressures. *Econ. Geol.* **46,** 821–835.

MOREY G. W., FORNIER R. O., and ROWE J. J. (1962) The solubility of quartz in water in the temperature interval from 25°C to 300°C. *Geochim. Cosmochim. Acta* **26,** 1029–1043.

MOSEBACH R. (1957) Thermodynamic behavior of quartz and other forms of silica in pure water at elevated temperatures and pressures with conclusions on their mechanism of solution. *J. Geol.* **65,** 347–363.

NOVGORODOV P. G. (1975) Quartz solubility in H_2O-CO_2 mixtures at 700°C and pressures of 3 and 5 kbars. *Geokhimica* **10,** 1484–1489.

PEACOCK S. M. (1993) The importance of blueschist → eclogite dehydration reactions in subducting oceanic crust. *GSA Bull.* **105,** 684–694.

PISTORIUS C. W. F. T., PISTORIUS M. C., BLAKELY J. P., and ADMIRAL L. J. (1963) Melting curve of Ice VII to 200 kbar. *J. Chem. Phys.*, **38,** 600–602.

PITZER K. S. (1983) Dielectric constant of water at very high temperature and pressure. *Natl. Acad. Sci. Proc.* **80,** 4575–4576.

QUIST A. S. (1970) The ionization constant of water to 800°C and 4000 bars. *J. Phys. Chem.* **74,** 3393–3402.

RICE M. H. and WALSH J. M. (1957) Equation of state of water to 250 kilobars. *J. Chem. Phys.* **26,** 824–830.

RIMSTIDT J. D. (1984) Quartz solubility at low temperatures. *GSA Abstr. Prog.* **16,** 635 (abstr.)

SACCOCIA P. J. and SEYFRIED W. E., JR. (1990) Talc-quartz equilibria and the stability of magnesium chloride complexes in NaCl-$MgCl_2$ solutions at 300, 350, and 400°C, 500 bars. *Geochim. Cosmochim. Acta* **54,** 3283–3294.

SAUL A. and WAGNER W. (1989) A fundamental equation for water covering the range from the melting line to 1273 K at pressures up to 25000 MPa. *J. Phys. Chem. Ref. Data* **18,** 1537–1564.

SAXENA S. K. and FEI Y. (1987a) High pressure and high temperature fluid fugacities. *Geochim. Cosmochim. Acta* **51,** 783–791.

SAXENA S. K. and FEI Y. (1987b) Fluids at crustal pressures and temperatures. *Contrib. Mineral. Petrol.* **95,** 370–375.

SHETTEL D. L., JR. (1974) The solubility of quartz in supercritical H_2O–CO_2 fluids. Ph.D. dissertation, Pennsylvania State Univ.

SHOCK E. L., HELGESON H. C., and SVERJENSKY D. A. (1989) Calculation of the thermodynamic and transport properties of aqueous species at high pressures and temperatures: Standard partial molal properties of inorganic neutral species. *Geochim. Cosmochim. Acta* **53,** 2157–2183.

SIEVER R. (1962) Silica solubility, 0°–200°C, and the diagenesis of siliceous sediments. *J. Geol.* **70,** 127–150.

SKOOG D. A., WEST D. M., and HOLLER F. J. (1994) *Analytical Chemistry* (sixth ed.). Harcourt Brace.

SOMMERFIELD R. A. (1967) Quartz solution reaction: 400–500°C, 1000 bars. *J. Geophys. Res.* **72,** 4253–4257.

STIXRUDE L. and BUKOWINSKI M. S. T. (1990) Fundamental thermodynamic relations and silicate melting with implications for the constitution of D″. *J. Geophys. Res.* **95,** 19,311–19,325.

SWEETON F. H., MESMER R. E., and BAES C. F., JR. (1974) Acidity measurements at elevated temperatures. VII. Dissociation of water. *J. Soln. Chem.* **3,** 191–214.

TANGER J. C. IV and HELGESON H. C. (1988) Calculation of the thermodynamic and transport properties of aqueous species at high pressures and temperatures: Revised equations of state for the standard partial molal properties of ions and electrolytes. *Amer. J. Sci.* **288,** 19–98.

VAN LIER J. A., DE BRUYN P. L., and OVERBEEK J. T. G. (1960) The solubility of quartz. *J. Phys. Chem.* **64,** 1675–1682.

WALTHER J. V. (1991) Determining the thermodynamic properties of solutes in crustal fluids. *Amer. J. Sci.* **291,** 453–472.

WALTHER J. V. and HELGESON H. C. (1977) Calculation of the thermodynamic properties of aqueous silica and the solubility of quartz and its polymorphs at high pressures and temperatures. *Amer. J. Sci.* **277,** 1315–1351.

WALTHER J. V. and ORVILLE P. M. (1983) The extraction-quench technique for determination of the thermodynamic properties of solute complexes: Application to quartz solubility in fluid mixtures. *Amer. Mineral.* **68,** 731–741.

WEILL D. F. and FYFE W. S. (1964) The solubility of quartz in H_2O in the range 1000–4000 bars and 400–550°C. *Geochim. Cosmochim. Acta* **28,** 1243–1255.

WOOD B. J. and WALTHER J. V. (1986) Fluid flow during metamorphism and its implications for fluid-rock ratios. In *Fluid-Rock Interaction During Metamorphism* (ed. J. V. WALTHER and B. J. WOOD), pp. 89–108. Springer-Verlag.

WYART J. and SABATIER G. (1955) Nouvelles mesures de la solubilité du quartz, de la tridymite et de la cristobalite dans l'eau sous pression au-dessus de la température critique. *Acad. Sci. Comptes Rendus* **240,** 1905–1907.

XIE Z. and WALTHER J. V. (1993) Quartz solubilities in NaCl solutions with and without wollastonite at elevated temperatures and pressures. *Geochim. Cosmochim. Acta* **57,** 1947–1955.